crystals

MDPI

Article

X-Ray Structures of Some Heterocyclic Sulfones

R. Alan Aitken *, David B. Cordes, Aidan P. McKay, Alexandra M. Z. Slawin and Dheirya K. Sonecha

EaStCHEM School of Chemistry, University of St Andrews, North Haugh, St Andrews, Fife KY16 9ST, UK
* Correspondence: raa@st-and.ac.uk; Tel.: +44-1334-463865

Abstract

1,4-Thiazine *S*,*S*-dioxide **1**, the *cis*- and *trans*-isomers **2** and **3** of its precursor 2,6-diethoxy-1,4-oxathiane *S*,*S*-dioxide, and diethyl 2,3-dihydro-1,4-thiazine-3,5-dicarboxylate *S*,*S*-dioxide **4** have been fully characterised, both in solution by ^{1}H and ^{13}C NMR and in the solid state by X-ray diffraction. Simulation has been used to model the unexpectedly complex ^{1}H NMR spectra and arrive at a full assignment of all chemical shifts and coupling constants. The crystal structures of both **1** and **4**, which adopt, respectively, boat and half-chair conformations, are dominated by strong NH to O=S hydrogen bonding leading to chains of molecules. In the case of **4**, the NMR data point to an equatorial position of the C(2)-ester group in solution, while in the crystal, this adopts an axial orientation. Compounds **2** and **3** adopt chair conformations both in solution and in the solid state with ring inversion on the NMR timescale leading to unexpected simplification of the spectra in the case of **3**.

Keywords: 1,4-thiazine *S*,*S*-dioxide; 1,4-oxathiane *S*,*S*-dioxide; NMR assignment; hydrogen bonding

1. Introduction

Some time ago, we described the X-ray structures of a range of ten symmetrical and unsymmetrical sulfones, but these were all acyclic [1]. More recently, we have reported the structures of some five-membered ring cyclic sulfones [2], as well as two examples of the heterocyclic 1,3-oxathiolane *S*,*S*-dioxides [3,4]. However, in general terms, the crystallographic investigation of heterocyclic sulfones remains an under-researched area, and there is ample scope for further studies, particularly in cases where the presence of a hydrogen-bond donor allows for the possibility of intermolecular hydrogen bonding.

Although there is one early claim to have isolated 1,4-thiazine as a stable liquid [5], this has never been reproduced and must be treated with scepticism. In the course of recent studies aimed at generation and isolation of this fundamental but hitherto unknown heterocyclic compound, we have prepared and characterised several related compounds, and we present here the structural characterisation of 1,4-thiazine *S*,*S*-dioxide **1**, *cis*-2,6-diethoxy-1,4-oxathiane *S*,*S*-dioxide **2**, *trans*-2,6-diethoxy-1,4-oxathiane *S*,*S*-dioxide **3**, and diethyl 3,4-dihydro-2*H*-1,4-thiazine-3,5-dicarboxylate *S*,*S*-dioxide **4** (Figure 1). Rather remarkably for such simple compounds, the extent of previous NMR characterisation is rather limited. Specifically, for **1**, **2,** and **3,** there are only low frequency ^{1}H spectra [6,7], and **4** is a previously unknown compound. We therefore also present here fully analysed and assigned ^{1}H and ^{13}C NMR data for all four compounds.

check for updates

Academic Editor: Thomas M. Klapötke

Received: 7 August 2025
Revised: 21 August 2025
Accepted: 22 August 2025
Published: 24 August 2025

Citation: Aitken, R.A.; Cordes, D.B.; McKay, A.P.; Slawin, A.M.Z.; Sonecha, D.K. X-Ray Structures of Some Heterocyclic Sulfones. *Crystals* **2025**, *15*, 750. https://doi.org/10.3390/cryst15090750

Copyright: © 2025 by the authors. Licensee MDPI, Basel, Switzerland. This article is an open access article distributed under the terms and conditions of the Creative Commons Attribution (CC BY) license (https://creativecommons.org/licenses/by/4.0/).

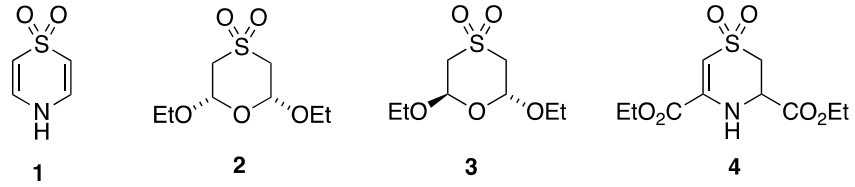


Figure 1. Structures of the four compounds studied.

2. Materials and Methods

2.1. Instrumentation and General Details

Melting points were recorded on a Reichert hot-stage microscope (Reichert, Vienna, Austria) and are uncorrected. NMR spectra were recorded in CD_3SOCD_3 for **1** and in $CDCl_3$ for **2–4** using Bruker AV 300, AV II 400 or AV III 500 instruments (Bruker, Billerica, MA, USA). Chemical shifts are reported in ppm to high frequency of the reference and are referenced to internal Me_4Si (δ 0.00) for ^1H and to the solvent signal (δ 39.50 CD_3SOCD_3, 77.00 $CDCl_3$) for ^{13}C, and coupling constants are in Hz. Spectra were processed and simulations performed using iNMR Reader version 6.3.3 (Mestrelab Research, Santiago de Compostela, Spain). Compound **6** was prepared as described [8]. A stream of ozone in oxygen was produced using a Fischer OZ 500/5 Ozone Generator (i-Fischer Engineering, Waldbüttelbrunn, Germany).

2.2. Synthesis of Sulfones **1–4**

2.2.1. Preparation of cis- and trans-2,6-diethoxy-1,4-oxathiolane 4,4-dioxide **2** and **3**

Following a literature procedure [6], ozone gas was passed into a solution of 3-sulfolene **5** (6 g, 50.8 mmol) in CH_2Cl_2 (50 cm^3) and ethanol (10 cm^3) cooled at −78 °C until a bubbler with potassium iodide in acetic acid in the exit gas stream indicated that ozone was no longer being absorbed. Liquid SO_2 (7 cm^3, 156 mmol) was then rapidly added, and the solution was stirred in the cold bath for 2 min before removing the bath and allowing it to stir at room temperature overnight. The resulting dark brown solution was poured into a vigorously stirred mixture of aqueous sodium carbonate (24 g in 200 cm^3 water) and 40 g of ice, and stirring continued for 5 min. The reaction mixture was poured into a separating funnel, and the CH_2Cl_2 layer was collected. The aqueous layer was washed with CH_2Cl_2 (2 × 50 cm^3), and the organic extracts were all combined. The combined layers were washed with water (1 × 60 cm^3) and saturated brine (1 × 60 cm^3), dried over magnesium sulfate, and the solvent evaporated *in vacuo* to yield the crude product as an off-white solid mixture (55:45) of the *cis* and *trans* isomers **2** and **3** (9.7 g, quant.), mp 75–130 °C (lit. [6] 76–118 °C). For the synthesis of **1,** this was used without further purification. However, in order to characterise the two isomers, they were separated by column chromatography (SiO_2, ethyl acetate/hexane 1:2) to give at R_f 0.6 (*cis* **2**) and at R_f 0.4 (*trans* **3**). The separated isomers were both recrystallised from methanol.

cis-2,6-diethoxy-1,4-oxathiolane 4,4-dioxide **2**

mp 102–105 °C (lit. [6] 103–105 °C); ^1H NMR (500 MHz, $CDCl_3$) δ 4.93 (2H, dd, *J* 9.5, 2.0, H-2, H-6), 3.99 (2H, dq, *J* 9.5, 7.0, OCH_2), 3.64 (2H, dq, *J* 9.5, 7.0, OCH_2), 3.25 (2H, dt, *J* 13.5, 2.0, H-3, H-5), 3.05 (2H, dd, *J* 13.5, 9.5, H-3, H-5) and 1.27 (6H, t, *J* 7.0, 2 × CH_3); ^{13}C NMR (125 MHz, $CDCl_3$) δ 95.1 (CH), 65.3 (OCH_2), 55.6 (SCH_2) and 14.9 (CH_3).

trans-2,6-diethoxy-1,4-oxathiolane 4,4-dioxide **3**

mp 134–136 °C (lit. [6] 136–137 °C); ^1H NMR (500 MHz, $CDCl_3$) δ 5.34 (2H, dd, *J* 5.5, 3.0, H-2, H-6), 3.91 (2H, dq, *J* 9.5, 7.0, OCH_2), 3.63 (2H, dq, *J* 9.5, 7.0, OCH_2), 3.30 (2H, ddd, *J* 14.0, 3.0, 2.0, H-3, H-5), 3.20 (2H, ddd, *J* 14.0, 5.5, 2.0, H-3, H-5) and 1.28 (6H, t, *J*

7.0, 2 × CH_3); ^{13}C NMR (125 MHz, $CDCl_3$) δ 93.4 (CH), 64.9 (OCH_2). 55.5 (SCH_2) and 14.8 (CH_3).

2.2.2. Preparation of 4*H*-1,4-Thiazine 1,1-dioxide **1**

Following a literature procedure [6], a mixture of 2,6-diethoxy-1,4-oxathiane 4,4-dioxides **2** and **3** (5 g, 22.3 mmol) and ammonium chloride (1.23 g, 23.3 mmol) in glacial acetic acid (100 cm^3) was heated under reflux for 30 min, during which the ammonium chloride dissolved, and the solution turned brownish yellow in colour. The mixture was then cooled to room temperature and the acetic acid evaporated off under reduced pressure to yield a yellow solid. This residue was stirred in a mixture of isopropanol (4 cm^3) and diethyl ether (25 cm^3) for 10 min. The suspension was then filtered, and the solid dried to yield the crude product **1**. Recrystallisation from MeOH yielded pure product **1** as yellow crystals (1.87 g, 55%), mp 239–243 °C (lit. [6] 237–240 °C). ^{1}H NMR (400 MHz, CD_3SOCD_3) δ 10.26 (1H, br s, NH), 7.09 (2H, m, H-3, H-5) and 5.99 (2H, m, H-2, H-6); ^{13}C NMR (100 MHz, CD_3SOCD_3) δ 132.6 (=CH-N) and 104.0 (S-CH=); HRMS (ESI) *m*/*z* calculated for $C_4H_4NO_2S$ [M–H] 129.9963, found 129.9960.

2.2.3. Preparation of diethyl 3,4-dihydro-2*H*-1,4-thiazine-3,5-dicarboxylate 1,1-dioxide **4**

Following a literature procedure [8], a solution of *m*-chloroperoxybenzoic acid (2.27 g, 13.16 mmol) in CH_2Cl_2 (10 cm^3) was added over the course of 5 min to a solution of diethyl 3,4-dihydro-2*H*-1,4-thiazine-3,5-dicarboxylate **6** (2.69 g, 10.97 mmol) in CH_2Cl_2 (30 cm^3) at –70 °C under nitrogen. The reaction was stirred at –70 °C for 20 min. After being warmed to room temperature, the reaction mixture was washed with $NaHCO_3$ (3 × 10 cm^3) and water (3 × 10 cm^3) and dried over $MgSO_4$. Evaporation of solvent *in vacuo* followed by purification using column chromatography (SiO_2, CH_2Cl_2 + 1% MeOH, R_f 0.3) produced the sulfoxide product **7** as an amber oil. (2.53 g, 88%); ^{1}H NMR (300 MHz, $CDCl_3$) δ 6.26 (1H, br s, =CH-), 4.35 (1H, m, -CH-NH-), 4.34 (4H, q, *J* 7, CH_2 of Et), 3.42 (1H, br d, *J* 13.4, H-2_a), 2.34 (1H, dd, *J* 13.5, 13.4, H-2_b) and 1.36 (6H, t, *J* 7, CH_3); ^{13}C NMR (125 MHz, $CDCl_3$) δ 170.1 (C=O, =C-CO_2Et), 161.5 (C=O, CH-CO_2Et), 137.8 (C), 96.2 (CH), 63.1 (OCH_2), 61.9 (OCH_2), 43.0 (CH-NH), 42.6 (SCH_2), 14.3 (CH_3) and 14.2 (CH_3). The ^{1}H and ^{13}C spectral data was in accordance with that previously reported [8].

A minor side-product obtained in earlier fractions (R_f 0.35) was diethyl 3,4-dihydro-2*H*-1,4-thiazine-3,5-dicarboxylate 1,1-dioxide **4** (0.15 g, 6%), mp 152–155 °C (dec.). IR (ATR): 3343, 2981, 1746, 1724, 1609, 1518, 1447, 1371, 1329, 1290, 1263, 1236, 1177, 1167, 1128, 1111, 1063, 1026, 1011 cm^{-1}; ^{1}H NMR ($CDCl_3$, 300 MHz) δ 6.14 (1H, br s, NH), 6.11 (1H, br s, =CH-), 4.67 (1H, ddd, *J* 12.3, 3.3, 1.7, CH-N), 4.36 (2H, q, *J* 7.0, OCH_2), 4.34 (2H, q, *J* 7.0, OCH_2), 3.53 (1H, dddd, *J* 13.2, 3.3, 2.4, 1.0, SCH_2) 3.17 (1H, dd, *J* 13.2, 12.3, SCH_2) 1.36 (3H, t, *J* 7.0, CH_3) and 1.35 (3H, t, *J* 7.0, CH_3); ^{13}C NMR ($CDCl_3$, 125 MHz) δ 167.4 (C=O, CH-CO_2Et), 161.2 (C=O, =C-CO_2Et), 138.0 (C), 100.4 (=CH), 63.3 (OCH_2), 63.1 (OCH_2), 52.7 (CH-N), 48.5 (SCH_2), 13.92 (CH_3) and 13.86 (CH_3); HRMS (ESI) *m*/*z* calculated for $C_{10}H_{15}NSO_6Na$ [M+Na] 300.0518, found 300.0507; calculated for $C_{20}H_{30}N_2S_2O_{12}Na$ [2M+Na] 577.1138, found 577.1121.

2.3. Crystallography

X-ray diffraction data for compound **1** were collected at 125 K using a Rigaku MM-007HF High Brilliance RA generator/confocal optics with XtaLAB P200 diffractometer [Cu Kα radiation (λ = 1.54187 Å)] (Rigaku Corporation, Tokyo, Japan). X-ray diffraction data for compounds **2** and **3** were collected at 125 K using a Rigaku FR-X Ultrahigh Brilliance Microfocus RA generator/confocal optics with XtaLAB P200 diffractometer [Mo Kα radiation (λ = 0.71073 Å)] (Rigaku Corporation, Tokyo, Japan). X-ray diffraction data for compound **4** were collected at 173 K using a Rigaku SCXmini CCD diffractometer with

a SHINE monochromator [Mo Kα radiation (λ = 0.71073 Å)] (Rigaku Corporation, Tokyo, Japan). Data for compounds **1–3** were collected (using a calculated strategy) and processed (including correction for Lorentz, polarization, and absorption) using CrysAlisPro [9], while data for **4** were collected using ω steps accumulating area detector images spanning at least a hemisphere of reciprocal space and processed (including correction for Lorentz, polarization, and absorption) using CrystalClear [10]. Structures were solved by either direct (SHELXS [11]) or dual-space methods (SHELXT [12]) with all structures refined by full-matrix least-squares against F^2 (SHELXL-2018/3 or 2019/3 [13]). Non-hydrogen atoms were refined anisotropically, and hydrogen atoms were refined using a riding model, except for the hydrogen atoms on N1 in **1** and **4,** which were located from the difference Fourier map and refined isotropically subject to a distance restraint. The terminal carbon (C8) of one ethoxy group in **3** was disordered over multiple sites related by rotations around the O2-C7 axis. The terminal carbon was split over three sites (36.5:31.2:32.3) and refined with their occupancies summed to 1 with restraints on the C-C distances and thermal ellipsoids. Calculations were performed using either the Olex2 [14] or CrystalStructure [15] interfaces. Selected crystallographic data are presented in Table 1. CCDC 2449906–2449909 contains the supplementary crystallographic data for this paper. These data can be obtained free of charge from The Cambridge Crystallographic Data Centre via www.ccdc.cam.ac.uk/structures.

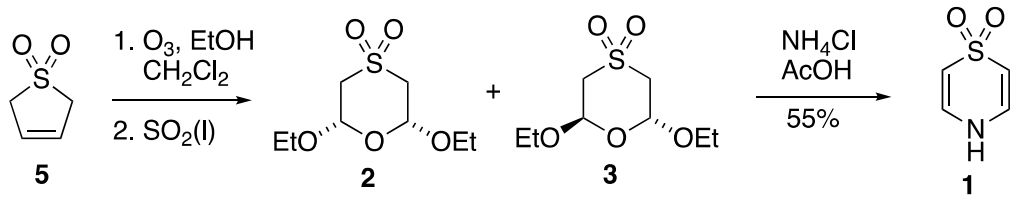
Table 1. Summary of crystallographic data obtained for compounds **1–4**.

Compound	**1**	**2**	**3**	**4**
CCDC deposit no.	2449906	2449907	2449908	2449909
Empirical formula	$C_4H_5NO_2S$	$C_8H_{16}O_5S$	$C_8H_{16}O_5S$	$C_{10}H_{15}NO_6S$
Crystal system	monoclinic	monoclinic	monoclinic	monoclinic
Space group	$P2_1/n$ (No. 14)	$P2_1/c$ (No. 14)	$I2/a$ (No. 15)	$P2_1/n$ (No. 14)
Temperature (K)	125	125	125	173
Crystal form	colourless plate	colourless plate	colourless plate	colourless prism
Size (mm)	0.08 × 0.04 × 0.008	0.30 × 0.16 × 0.03	0.18 × 0.12 × 0.02	0.17 × 0.07 × 0.07
a (Å)	6.8189(2)	9.26086(15)	9.05992(12)	5.5089(3)
b (Å)	9.9891(3)	13.2940(2)	12.75336(18)	19.7489(13)
c (Å)	8.3841(3)	8.58184(14)	19.5748(3)	11.5347(8)
β (°)	110.087(4)	96.5134(15)	95.2016(13)	100.1790(10)
Volume (Å^3)	536.34(3)	1049.72(3)	2252.44(6)	1235.16(14)
Z	4	4	8	4
D_c (g cm^{-3})	1.624	1.419	1.323	1.491
Absorption coefficient (mm^{-1})	4.560	0.304	0.283	0.282
Radiation type, wavelength (Å)	Cu *Kα*, 1.54187	Mo *Kα*, 1.71073	Mo *Kα*, 1.71073	Mo *Kα*, 1.71073
F(000)	272.00	480.00	960.00	584.00
θ range (°)	7.161–75.646	2.213–29.151	1.908–29.214	2.069–27.479
Limiting indices	−8 ≤ h ≤ 8, −12 ≤ k ≤ 12, −10 ≤ l ≤ 10	−12 ≤ h ≤ 12, −17 ≤ k ≤ 18, −11 ≤ l ≤ 11	−12 ≤ h ≤ 12, −17 ≤ k ≤ 16, −26 ≤ l ≤ 26	−7 ≤ h ≤ 7, −25 ≤ k ≤ 25, −14 ≤ l ≤ 14
Reflns collected/unique	8448/1098	44,431/2673	46,039/2858	12,586/2822
R_{int}	0.0565	0.0343	0.0547	0.1003
Restraints/parameters	1/77	0/129	19/152	1/169
Data with $I > 2\sigma(I)$	926	2422	2486	1747
Goodness of fit on F^2	1.100	1.062	1.069	1.021
R_1, wR_2 (data $I > 2\sigma(I)$)	0.0459, 0.1111	0.0286, 0.0750	0.0410, 0.1023	0.0497, 0.0946
R_1, wR_2 (all data)	0.0572, 0.1200	0.0322, 0.0769	0.0512, 0.1054	0.1060, 0.1160
Largest diff. peak/hole (e Å^2)	0.39 and −0.44	0.40 and −0.36	0.75 and −0.21	0.38 and −0.40

3. Results and Discussion

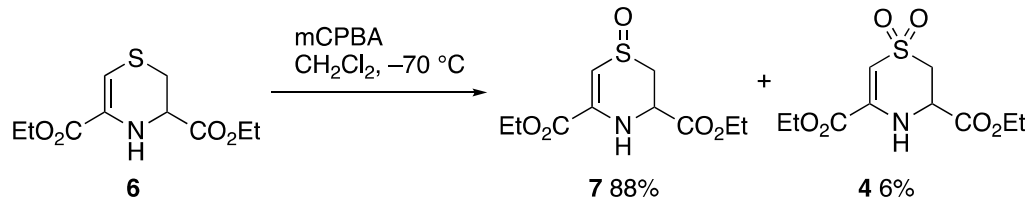
3.1. Synthesis

A reliable although unusual synthesis of compound **1** appeared in 1972 [6], and in fact, this is its only reported synthesis to date. The method starts from the readily available 2,5-dihydrothiophene 1,1-dioxide (butadiene sulfone) **5,** which is subjected to ozonolysis in dichloromethane containing ethanol (Scheme 1). Once ozone absorption is complete, the mixture is reductively quenched by rapid addition of liquid sulfur dioxide to give a mixture of the *cis*- and *trans*-2,6-diethoxy-1,4-oxathiane 4,4-dioxides **2** and **3** in essentially quantitative yield. Treatment of this mixture with ammonium chloride in boiling acetic acid directly produced thiazine dioxide **1**, but for spectroscopic and structural characterisation, **2** and **3** were readily separated by column chromatography. It might be noted here that compound **3** has been prepared in low yield by treatment of sulfonyldiacetaldehyde with boron trifluoride and ethanol [16], and both **2** and **3** have also been prepared by peracetic acid oxidation of the corresponding 1,4-oxathianes [7].



Scheme 1. Synthetic route to compounds **1**, **2,** and **3** [6].

Compound **4** was obtained as a minor product in the low-temperature mCPBA oxidation of the dihydrothiazine diester **6** (Scheme 2), itself obtained by condensation of cysteine ethyl ester with ethyl bromopyruvate [8]. Chromatography of the product yielded sulfone **4** as a minor product eluting before the main sulfoxide product **7**.



Scheme 2. Synthetic route to compound **4**.

*3.2. NMR Characterisation of Compounds **1–4***

Because of the early date of the previous work, only low-resolution ^{1}H spectra of compounds **1–3** were reported [6,7], although a later study [17] did attempt assignment of coupling constants for the ^{1}H spectrum of **1** and also gave ^{13}C chemical shifts for **1**. No ^{13}C NMR data for **2** or **3** seem to have been reported, and compound **4** is previously unknown, so no spectroscopic data exist. We therefore conducted a detailed NMR study of compounds **1–4,** and the resulting chemical shift values with assignments are summarised in Figure 2. All spectra including simulations are presented in the Supplementary Materials. By using DEPTQ and HSQC techniques, unambiguous assignment of all carbon signals was possible for all four compounds, with the sole exception of the CH_3 signals in **4**. Unambiguous assignment of the OCH_2 signals was possible in this case from observation of an HMBC correlation of the carbon signal at 161.2 to the proton signals at both 6.11 and 4.36, whilst the signal at 167.4 was only correlated to the signal at 4.34. HSQC then confirmed that 4.36 corresponded to 63.3, while 4.34 corresponded to 63.1.

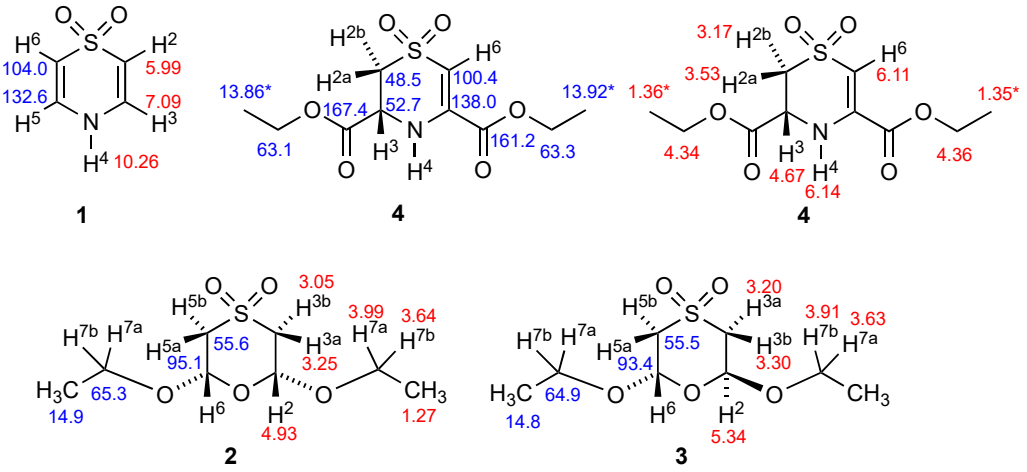


Figure 2. Structures of compounds **1–4** with ^{1}H (red) and ^{13}C (blue) NMR chemical shifts and numbering system used for Table 2. (* Assignments within **4** may be interchanged).

Table 2. H–H coupling constants observed in **1–4** (Hz).

Compound	$^{2}J_{H\text{-}H}$	$^{3}J_{H\text{-}H}$	$^{4}J_{H\text{-}H}$
1 *	—	H^2-H^3 = H^5-H^6 = 10.0 H^3-H^4 = H^4-H^5 = 6.6	H^2-H^6 = 1.8 H^3-H^5 = 4.4 H^2-H^4 = H^4-H^6 = 1.2
2	H^{3a}-H^{3b} = H^{5a}-H^{5b} = 13.5 H^{7a}-H^{7b} = 9.5	H^2-H^{3a} = H^{5a}-H^6 = 9.5 H^2-H^{3b} = H^{5b}-H^6 = 2.0 H^{7a}-CH_3 = H^{7b}-CH_3 = 7.0	H^{3a}-H^{5a} = 2.0
3	H^{3a}-H^{3b} = H^{5a}-H^{5b} = 14.0 H^{7a}-H^{7b} = 9.5	H^2-H^{3a} = H^{5a}-H^6 = 5.5 H^2-H^{3b} = H^{5b}-H^6 = 3.0 H^{7a}-CH_3 = H^{7b}-CH_3 = 7.0	H^{3a}-H^{5b} = H^{3b}-H^{5a} = 2.0
4	H^{2a}-H^{2b} = 13.2	H^{2a}-H^3 = 12.3 H^{2b}-H^3 = 3.3 H^3-H^4 = 1.7 CH_2-CH_3 = 7.0	H^{2a}-H^4 = 2.4 H^{2a}-H^6 = 1.0

* $^{5}J_{H2\text{-}H5}$ = $^{5}J_{H3\text{-}H6}$ = 0.4.

The other feature of interest from the NMR spectra was the presence of only four carbon environments in both **2** and **3,** thus confirming their symmetry with a mirror plane in **2** and a C-2 axis in **3**. As will be seen from the X-ray structures, both these molecules exist in chair forms in the solid state, and, for **3**, this places one OEt axial and the other equatorial. However, in solution, there is clearly rapid inversion on the NMR timescale, which results in the axial OEt becoming equatorial and vice versa, thus resulting in averaging to give the simple four-line spectrum. For **2,** the contribution of the chair form with two axial OEt groups is negligible, again leading to only four lines.

While the ^{13}C spectra for all four compounds were relatively simple, this was certainly not the case for the ^{1}H spectra, which showed remarkable complexity for such simple structures. To take compound **1** as an example, while the NH signal was observed as a broad singlet at 10.26 ppm, the complex form of the CH signals is shown in Figure 3.

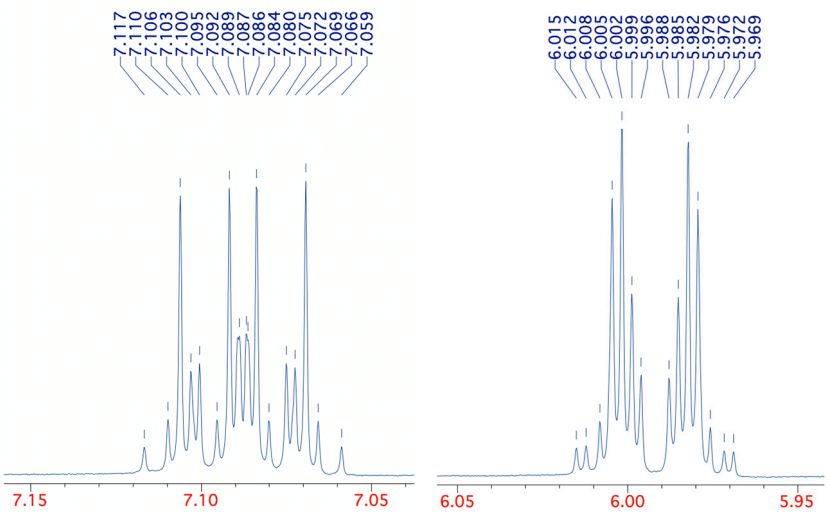


Figure 3. Detailed form of the 400 MHz ^{1}H NMR CH signals for compound **1**.

This pattern could be successfully simulated, however, using the precise chemical shifts of 7.088 and 5.992 and the coupling constants in Table 2. With these values, we were able to reproduce the pattern exactly with the same number and relative size of peaks and all 32 chemical shifts agreeing to ±0.002 ppm (see Supplementary Materials). The complexity of the patterns for the simple AA'MM'X system is explained by a total of six different coupling constants, including between chemically equivalent but magnetically non-equivalent protons H^2/H^6 and H^3/H^5 and even a weak five-bond coupling diagonally across the ring. The values are also in reasonable agreement with those previously reported [17], although in that case, no coupling to NH was apparently observed.

The spectra of compounds **2** and **3** also showed unexpected complexity but for a different reason: in this case, the CH_2 protons of the OEt groups as well as those on the ring were non-equivalent and coupled to one another. In addition, for the *cis* compound **2,** there was a four-bond coupling between the magnetically non-equivalent protons H^{3a}/H^{5a}, which being equatorial form a W-shape favourable for long-range coupling. Again, satisfactory simulation was possible with agreement to ±0.001 ppm on all peaks using the values in Table 2. A similar pattern was observed for the *trans* compound **3** with the distinction that in this case, four-bond coupling was observed between the chemically non-equivalent H^{3a}/H^{5b} and H^{3b}/H^{5a} pairs, each of which can take up the favourable W-shape in one of the rapidly interconverting chair forms.

The spectrum of the unsymmetrical compound **4** was somewhat simpler and was consistent with a half-chair conformation with the 3-CO_2Et substituent taking up an equatorial position. This leads to a large diaxial coupling between H^3 and H^{2b} and places H^{2a} in an equatorial position allowing favourable W-shape long-range coupling to both the =CH hydrogen and the NH (Table 2).

3.3. Molecular and Crystal Structures of ***1–4*** *from X-Ray Diffraction*

The molecular structure of **1** is almost but not quite planar, showing a slight boat shape with N1 0.040(4) and S4 0.093(4) Å below the plane defined by the four carbon atoms (Figure 4). More significantly, the sulfone function is distinctly unsymmetrical with one shorter bond S4–O4 of 1.442(2) Å placing O4 1.022(6) Å above the carbon atom plane and one longer bond S4–O3 of 1.453(3) Å placing O3 1.383(6) Å below it. This is explained by strong intermolecular hydrogen bonding between O3 and the NH (Table 3), which results in the molecules forming infinite zig-zag chains when viewed along the *a*-axis and additional non-classical hydrogen bonds from C3 and C5 (Table 3), which link adjacent intermolecular chains.

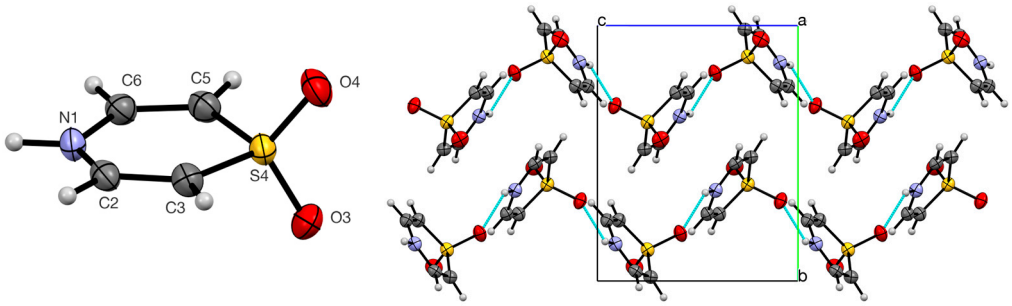


Figure 4. Molecular structure of **1** showing numbering system used (50% probability ellipsoids) and hydrogen bonding pattern (blue dashed lines) in the crystal viewed along the *a*-axis.

Table 3. Hydrogen bonding (including non-classical) parameters for **1** and **4** (Å, °).

	D—H···A	D—H	H···A	D···A	D—H···A
1	N(1)–H(1)···O(3)#1	0.952(18)	2.11(3)	2.851(3)	134(3)
	C(3)-H(3)···O(3)#2	0.95	2.551(3)	3.408(4)	150.1(2)
	C(5)-H(5)···O(3)#3	0.95	2.5029(18)	3.260(4)	136.61(19)
4	N(1)–H(1)···O(3)#4	0.98(3)	2.10(3)	2.887(3)	136(2)

Symmetry codes: #1 x − 1/2, −y + 3/2, z + 1/2; #2 − x, −y + 1, z; #3 x + 1/2, −y +3/2, z + 1/2; #4 x + 1/2, −y + 1/2, z − 1/2.

The bond lengths and angles around the heterocyclic ring (Table 4) are in good agreement with those reported for the four 1,4-thiazine *S*,*S*-dioxides that have previously been crystallographically characterised (Figure 5). The first three of these also exhibit hydrogen bonding between NH and one of the sulfone oxygens: the diphenyl compound **8** forms hydrogen-bonded stacks [18], the bis(difluoromethyl) compound **9** forms linear hydrogen-bonded chains [19] and the 2-pyridyl compound **10** forms linear chains with an additional intramolecular hydrogen-bonding interaction with the pyridyl N [20]. The *N*-acetyl compound **11** has ring dimensions most similar to **1,** but no hydrogen bonding is possible in this case, and there are no significant intermolecular interactions in the crystal [21].

Table 4. Comparison of key ring dimensions between the four compounds (Å, °).

Bond Length	**1**	**2**	**3**	**4**
N/O(1)–C(2)	1.352(4)	1.4307(12)	1.4379(16)	1.348(3)
C(2)–C(3)	1.351(4)	1.5265(14)	1.518(2)	1.350(4)
C(3)–S(4)	1.711(3)	1.7761(11)	1.7670(15)	1.718(3)
S(4)–C(5)	1.713(3)	1.7799(11)	1.7734(14)	1.770(3)
C(5)–C(6)	1.342(4)	1.5256(14)	1.526(2)	1.531(3)
C(6)–N/O(1)	1.361(4)	1.4297(12)	1.4283(16)	1.448(3)
S(4)–O(3)	1.453(2)	1.4402(9)	1.4382(12)	1.4439(19)
S(4)–O(4)	1.442(2)	1.4455(9)	1.4433(11)	1.439(2)
Angle				
C(6)–N/O(1)–C(2)	122.5(2)	113.22(8)	115.38(10)	123.5(2)
N/O(1)–C(2)–C(3)	124.3(3)	110.86(8)	110.56(11)	126.3(2)
C(2)–C(3)–S(4)	123.3(2)	110.71(7)	110.06(10)	121.0(2)
C(3)–S(4)–C(5)	101.58(15)	102.29(5)	101.00(7)	101.13(13)
S(4)–C(5)–C(6)	123.1(3)	109.00(7)	113.86(9)	110.51(18)
C(5)–C(6)–N/O(1)	124.7(3)	109.40(8)	112.55(11)	111.6(2)

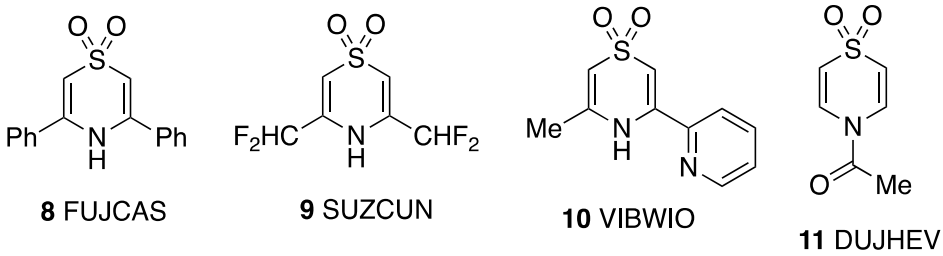


Figure 5. Other crystallographically characterised 1,4-thiazine *S*,*S*-dioxides with CSD Refcodes.

The molecular structures of the *cis* compound **2** and the *trans* compound **3** both adopt a regular chair conformation, with both ethoxy groups equatorial in the first case and one equatorial and one axial in the second (Figure 6). There is some rotational disorder in the equatorial ethoxy group for **3** with the methyl group occupying two alternative sites in addition to the one shown. In both structures, there are a variety of weak CH···O interactions (2.4403(8)–2.8017(9) Å and 2.3650(10)–2.7824(10) Å, respectively) which are at or beyond the sum of the Van der Waals radii.

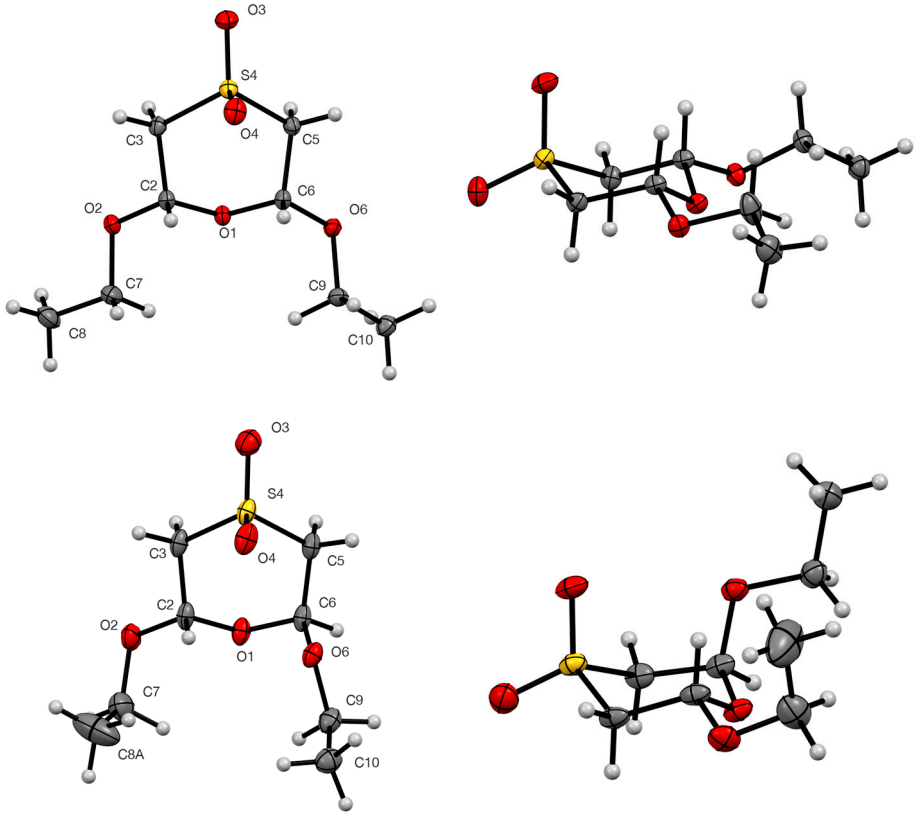


Figure 6. Molecular structures of **2** (**top**) and **3** (**bottom**) showing numbering system used (50% probability ellipsoids). The minor components of disorder in **3** are omitted for clarity.

The bond lengths and angles around the heterocyclic rings (Table 4) are in good agreement with those reported for the three 1,4-oxathiane *S*,*S*-dioxides that have previously been crystallographically characterised (Figure 7). Compound **12** also adopts a chair conformation with all substituents equatorial, while the isomer **13** has the adjacent methoxy and ethoxy groups both axial and the remaining ethoxy equatorial [22]. The structure of the *trans* dimethoxy compound **14** [23] is exactly analogous to that of **3** with one group axial and one equatorial. As might be expected, none of these compounds show significant intermolecular interactions.

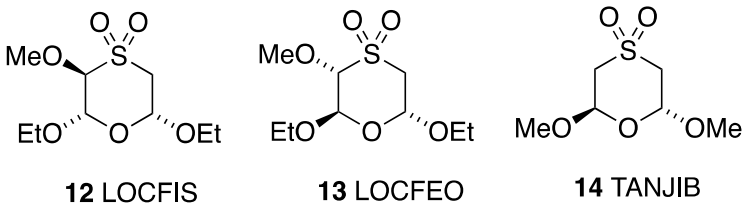


Figure 7. Other crystallographically characterised 1,4-oxathiane *S*,*S*-dioxides with CSD Refcodes.

The dihydro-1,4-thiazine *S*,*S*-dioxide diester **4** adopts a half-chair conformation in the crystal with N(1), C(2), C(3), and S(4) as well as the C-2 ester group in a plane, with C(5) significantly (0.659(4) Å) below it while C(6) is slightly(0.071(4) Å) above it. The C-6 ester group adopts an axial position (Figure 8). The cyclic amine NH is involved in both an electrostatic-type intermolecular interaction with the C=O of the in-plane C-2 ester group and an intermolecular hydrogen bond to the S=O(3) of an adjacent molecule (Table 3) leading to chains perpendicular to the *b* axis with two alternating molecular orientations (Figure 8, Table 3).

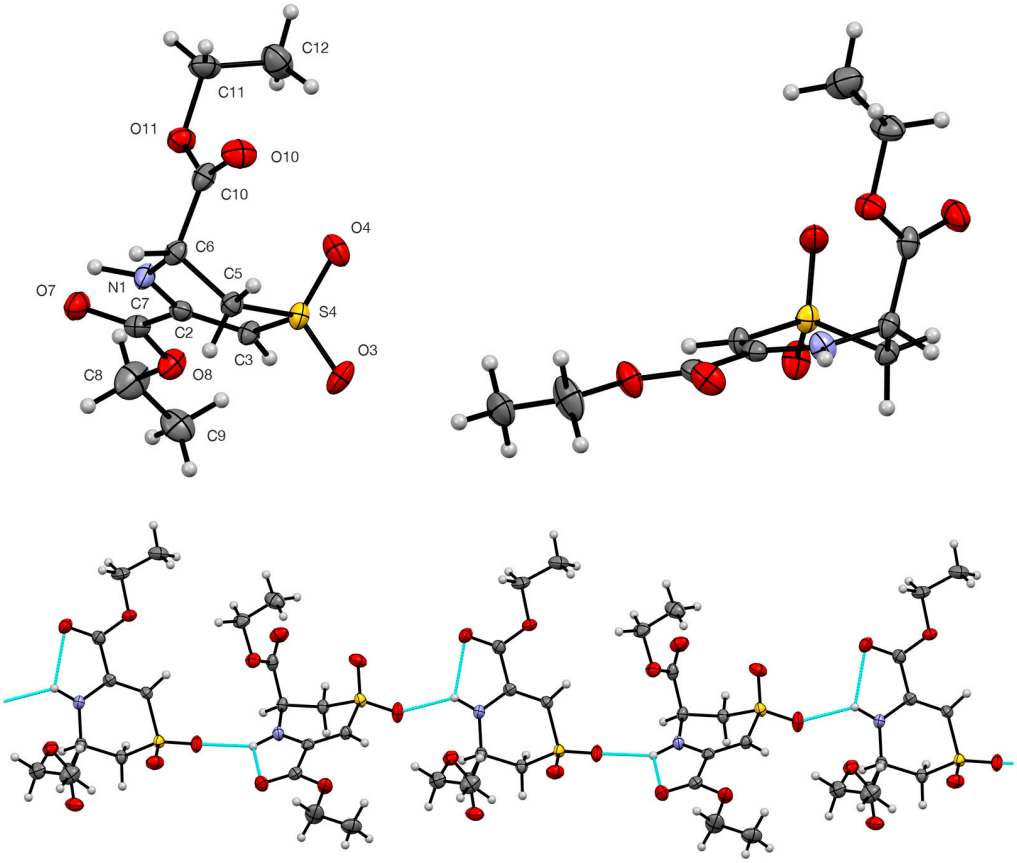


Figure 8. Molecular structure of **4** showing numbering system used (50% probability ellipsoids) and hydrogen bonding pattern (blue dashed lines) in the crystal viewed along the *b* axis.

It is notable that the axial orientation of the C(6)-ester group in the crystal structure is not in agreement with the NMR data presented earlier, which clearly indicated an equatorial ester group, and we conclude that the molecule adopts different conformations in the solid state and in solution.

A good number of structures containing a 2,3-dihydro-1,4-thiazine *S*,*S*-dioxide ring have been determined (Figure 9), but these almost all have two or more additional rings fused to the thiazine double bond and no substituent at the 3-position adjacent to NH. The interest in these structures stems from their isolation as natural products from marine

sources and potential medicinal activity. Thus, euthyroideone A **15** [24] was obtained from a New Zealand bryozoan, while ascidiathiazone A **16** [25] was obtained from a New Zealand ascidian, and both it and its analogue **17** [26] were tested for anti-inflammatory activity. The regioisomers xestosaprol O **18** and xestosaprol N **19** isolated from a Micronesian marine sponge are inhibitors of indoleamine 2,3-dioxygenase [27]. The compound **20** is an intermediate in the synthesis of the core structure of antimalarial thiaplakortone analogues [28], and the same group also determined the structure of an intermediate **21** with the regioisomeric ring system [29]. The structural parameters of the dihydrothiazine ring in all these examples are in good agreement with those for **4** with the same half-chair conformation in each case. These examples show a range of interesting hydrogen bonding patterns, but these generally involve bonding of NH to a carbonyl oxygen rather than to sulfone SO. In compound **20,** however, there is intermolecular NH to sulfone SO bonding forming cyclic tetramers.

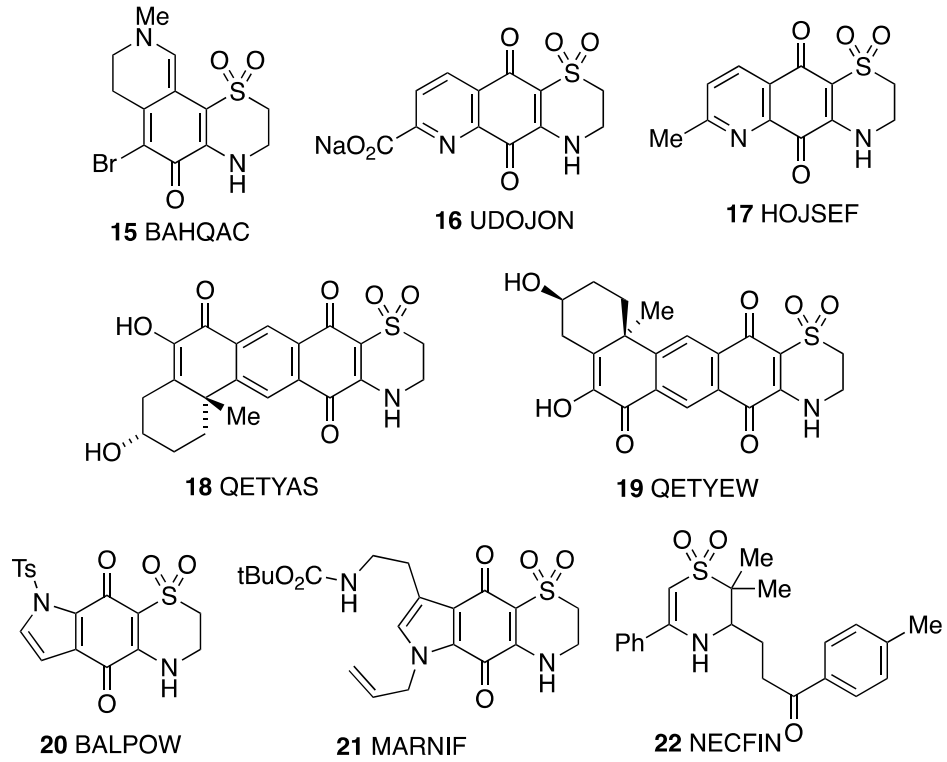


Figure 9. Other crystallographically characterised 2,3-dihydro-1,4-thizine *S*,*S*-dioxides with CSD Refcodes.

Perhaps the most relevant example for comparison with **4** is the monocyclic compound **22** obtained as a by-product in studies on the radical sulfonylative cyclisation of alkenes [30]. Like compound **4,** this has a half-chair conformation, but in contrast to **4,** the large benzoylethyl substituent in **22** is equatorial. This compound also forms chains by intermolecular NH to sulfone SO hydrogen bonding, as does **4**.

4. Conclusions

Valuable structural information has been obtained on the four compounds studied, both in solution using NMR and in the solid state by X-ray crystallography. The intermolecular NH to O=S hydrogen bonding observed in the structures of **1** and **4** is consistent with the pattern observed for previously determined structures of these ring systems. The unexpectedly complex ^{1}H NMR pattern observed for **1** can be explained by invoking long-range coupling through four and five bonds. For the oxathiane dioxides **2** and **3,** the

data are consistent with chair conformations both in solution and in the solid state. Perhaps unexpectedly, the sp^3-linked ester group in **4** adopts an equatorial position in solution but an axial position in the crystal.

Supplementary Materials: The following supporting information can be downloaded at https://www.mdpi.com/article/10.3390/cryst15090750/s1: full NMR spectra for **1–4** (Figures S1–S20).

Author Contributions: D.K.S. prepared the compounds; D.B.C. and A.P.M. (cpd **1–3**) or A.M.Z.S. (cpd **4**) collected the X-ray diffraction data and solved the structures; R.A.A. devised the study, supervised the work, analysed the data, and wrote the paper. All authors have read and agreed to the published version of the manuscript.

Funding: This research received no external funding.

Data Availability Statement: All X-ray diffraction data has been deposited at the Cambridge Crystallographic Data Centre with Deposit Nos. 2449906–2449909 as detailed in Table 1 and can be obtained free of charge via www.ccdc.cam.ac.uk/structures, and research data supporting this publication (original NMR files) can be accessed at https://doi.org/10.17630/43f20988-0372-46b0-8017-98bc06dbd532.

Conflicts of Interest: The authors declare no conflicts of interest.

References

1. Rudolph, F.A.M.; Fuller, A.L.; Slawin, A.M.Z.; Bühl, M.; Aitken, R.A.; Woollins, J.D. The X-ray structures of sulfones. *J. Chem. Crystallogr.* **2010**, *40*, 253–265. [CrossRef]
2. Aitken, R.A.; Slawin, A.M.Z.; Sonecha, D.K. The X-ray structures of 2- and 3-sulfolene and two halogenated derivatives. *J. Chem. Crystallogr.* **2023**, *53*, 431–437. [CrossRef]
3. Aitken, R.A.; Lightfoot, P.; Thomas, A.W. Synthesis, structure and reactivity of some chiral benzylthio alcohols, 1,3-oxathiolanes and their *S*-oxides. *J. Sulfur Chem.* **2020**, *41*, 369–387. [CrossRef]
4. Aitken, R.A.; Henderson, S.; Slawin, A.M.Z. Structure and thermal reactivity of some 2-substituted 1,3-oxathiolane *S*-oxides. *J. Sulfur Chem.* **2018**, *39*, 422–434. [CrossRef]
5. Barkenbus, C.; Landis, P.S. The Preparation of 1,4-Thiazine. *J. Am. Chem. Soc.* **1947**, *70*, 684–685. [CrossRef]
6. Noland, W.E.; DeMaster, R.D. 4*H*-1,4-Thiazine 1,1-dioxide. *Org. Synth.* **1972**, *52*, 135–138. [CrossRef]
7. Lopez Aparicio, F.J.; Zorrilla Benitez, F.; Santoyo Gonzalez, F. Acetals and thioacetals from thioglycolaldehyde: Some oxidation products. *Carbohydr. Res.* **1982**, *110*, 195–205. [CrossRef]
8. Berges, D.A.; Taggart, J.J. A spontaneous sulfoxide dehydration. *J. Org. Chem.* **1985**, *50*, 413–415. [CrossRef]
9. *CrysAlisPro*; v1.171.42.94a & 96a; Rigaku Oxford Diffraction; Rigaku Corporation: Tokyo, Japan, 2023.
10. *CrystalClear-SM Expert*; v2.1.; Rigaku Americas: The Woodlands, TX, USA; Rigaku Corporation: Tokyo, Japan, 2015.
11. Sheldrick, G.M. A short history of SHELX. *Acta Crystallogr. Sect. A: Found. Adv.* **2008**, *64*, 112–122. [CrossRef]
12. Sheldrick, G.M. SHELXT—Integrated space-group and crystal structure determination. *Acta Crystallogr. Sect. A: Found. Adv.* **2015**, *71*, 3–8. [CrossRef] [PubMed]
13. Sheldrick, G.M. Crystal structure refinement with SHELXL. *Acta Crystallogr. Sect. C: Struct. Chem.* **2015**, *71*, 3–8. [CrossRef]
14. Dolomanov, O.V.; Bourhis, L.J.; Gildea, R.J.; Howard, J.A.K.; Puschmann, H. OLEX2: A complete structure solution, refinement and analysis program. *J. Appl. Crystallogr.* **2009**, *42*, 339–341. [CrossRef]
15. *CrystalStructure*; v4.3.0.; Rigaku Americas: The Woodlands, TX, USA; Rigaku Corporation: Tokyo, Japan, 2018.
16. McCormick, J.E.; McElhinny, R.S. 3-Heteraglutaraldehydes. Part II. Tetrahydrothiophen-3,4-diol 1,1-dioxides and the chemistry of their oxidation product, 3-thiaglutaraldehyde 3,3-dioxide, and its derivatives. *J. Chem. Soc. Perkin Trans. 1* **1972**, 1335–1342. [CrossRef]
17. Fraenkel, G.; Kolp, C.J.; Chow, A. Theoretical and experimental studies of cycloconjugation involving second-row elements. *J. Am. Chem. Soc.* **1992**, *114*, 4307–4314. [CrossRef]
18. Chang, M.-Y.; Lin, C.-Y. Construction of diaryl oxacyclic sulfones via $Bi(OTf)_3$-catalyzed intramolecular cyclocondensation of 1,3-diaroylsulfones. *Org. Bimol. Chem.* **2025**, *23*, 1662–1672. [CrossRef]
19. Ogurok, V.M.; Siry, S.A.; Rusanov, E.B.; Vlasenko, Y.G.; Shermolovich, Y.G. Synthesis of symmetrical 3,5-bis(difluoromethyl)-1,4-thiazine 1,1-dioxides. *J. Fluor. Chem.* **2016**, *182*, 47–52. [CrossRef]
20. Ladouceur, S.; Donato, L.; Romain, M.; Mudraboyina, B.P.; Johansen, M.B.; Wisner, J.A.; Zysman-Colman, E. A rare case of dual emission in a neutral heteroleptic iridium(III) complex. *Dalton Trans.* **2013**, *42*, 8838–8847. [CrossRef] [PubMed]

21. Fraenkel, G.; Chow, A.; Gallucci, J.; Rizvi, S.Q.A.; Wong, S.C.; Finkelstein, H. Demonstration of heteroaromaticity via d-orbital overlap in a cyclic conjugated sulfone: NMR, crystallography, and ab initio calculation. *J. Am. Chem. Soc.* **1986**, *108*, 5339–5341. [CrossRef]
22. Roversi, E.; Monnat, F.; Schenk, K.; Vogel, P.; Braña, P.; Sordo, J.A. ^{17}O NMR spectroscopy of sulfolenes (2,5-dihydrothiophene 1,1-dioxides) and sultines (3,6-dihydro-1,2-oxathiin 2-oxides)—Experiment and quantum calculations: Synthesis of 4,9-dioxo-1,2-oxathiacyclodecane 2-oxide, a new heterocycle. *Chem. Eur. J.* **2000**, *6*, 1858–1864. [CrossRef]
23. Estrada, M.D.; López-Castro, A. Structure of 2,6-dimethoxy-1,4-oxathiane 4,4-dioxide. *Acta Crystallogr. Sect. C: Cryst. Struct. Commun.* **1991**, *47*, 1030–1032. [CrossRef]
24. Morris, B.D.; Prinsep, M.R. Euthyroideones, novel brominated quinone methides from the bryozoan *Eurythroides episcopalis*. *J. Org. Chem.* **1998**, *63*, 9545–9547. [CrossRef]
25. Pearce, A.N.; Chia, E.W.; Berridge, M.V.; Clark, G.R.; Harper, J.L.; Larsen, L.; Maas, E.W.; Page, M.J.; Perry, N.B.; Webb, V.L.; et al. Anti-inflammatory thiazine alkaloids isolated from the New Zealand ascidian *Aplidium* sp.: Inhibitors of the neutrophil respiratory burst in a model of gouty arthritis. *J. Nat. Prod.* **2007**, *70*, 936–940. [CrossRef]
26. Chia, E.W.; Pearce, A.N.; Berridge, M.V.; Larsen, L.; Perry, N.B.; Sansom, C.E.; Godfrey, C.A.; Hanton, L.R.; Lu, G.-L.; Walton, M.; et al. Synthesis and anti-inflammatory structure-activity relationships of thiazine-quinoline-quinones: Inhibitors of the neutrophil respiratory burst in a model of acute gouty arthritis. *Bioorg. Med. Chem.* **2007**, *16*, 9432–9442. [CrossRef] [PubMed]
27. Shi, Y.; Ji, Y.; Xin, K.; Gao, S. Total synthesis of (–)-xestosaprol N and O. *Org. Lett.* **2018**, *20*, 732–735. [CrossRef]
28. Schwartz, B.D.; Coster, M.J.; Skinner-Adams, T.S.; Andrews, K.T.; White, J.M.; Davis, R.A. Synthesis and antiplasmodial evaluation of analogues based on the tricyclic core of thiaplakortones A–D. *Mar. Drugs* **2015**, *13*, 5784–5795. [CrossRef] [PubMed]
29. Schwartz, B.D.; Coster, M.J.; Davis, R.A.; Healy, P.C. *CSD Communication*; Cambridge Crystallographic Data Centre: Cambridge, UK, 2017; MARNIF.
30. Mao, R.; Yuan, Z.; Li, Y.; Wu, J. *N*-Radical-initiated cyclization through insertion of sulfur dioxide under photoinduced catalyst-free conditions. *Chem. Eur. J.* **2017**, *23*, 8176–8179. [CrossRef] [PubMed]

Disclaimer/Publisher's Note: The statements, opinions and data contained in all publications are solely those of the individual author(s) and contributor(s) and not of MDPI and/or the editor(s). MDPI and/or the editor(s) disclaim responsibility for any injury to people or property resulting from any ideas, methods, instructions or products referred to in the content.